Mean field study of the quadrupole-octupole degree of freedom in the *spdf* boson model

Serdar Kuyucak
Department of Theoretical Physics, Research School of Physical Sciences, Australian National University, Canberra ACT 0200, Australia

Michio Honma
Center for Mathematical Sciences, University of Aizu, Tsuruga, Ikki-machi Aizu-Wakamatsu, Fukushima 965-8580, Japan
(Received 22 March 2002; published 20 June 2002)

We present a mean field study of the quadrupole-octupole degree of freedom in collective nuclei within the framework of the *spdf*-boson model. For realistic choices of the Hamiltonian parameters, the ground state of the system is shown to remain axially symmetric, which considerably simplifies the mean field treatment. The critical point for the onset of octupole deformation in quadrupole deformed systems is identified in the parameter space and importance of the parity projection in this process is emphasized. A systematic survey of excitation energies and electric transitions for one-phonon states is given, which will provide useful guidance for detailed studies of negative parity states within the *spdf*-boson model.

DOI: 10.1103/PhysRevC.65.064323 PACS number(s): 21.60.Ev, 21.60.Fw, 23.20.Js, 27.90.+b

I. INTRODUCTION

The low-lying negative parity states in even-even collective nuclei are described in terms of the octupole degree of freedom (see Refs. [1–3] for reviews). From the early stages, the octupole degree of freedom has been incorporated in the interacting boson model (IBM) [4] by coupling a single octupole, f boson to the sd-boson system [5]. Because of its simplicity, this formalism has been very popular in applications of the IBM to negative parity states and continues to provide a useful framework for analysis of octupole vibrations in deformed nuclei (see Refs. [6–8] for systematic studies). However, due to the weak coupling assumption inherent in the truncation of the basis to a single f boson, it is limited to a description of octupole vibrations and the formalism needs to be extended to a full sdf basis for discussion of octupole deformations.

In a parallel development, the necessity of including p bosons in description of octupole deformed systems was emphasized in several studies from very different perspectives. From the point of view of dynamical symmetries, the symmetry group of the sdf-boson system U(13) does not contain SU(3), the limit associated with deformed systems, but U(16) of the $spdf$-boson system does [9]. In the SU(3) limit of the $spdf$-IBM, the p and f bosons are treated on an equal footing and have degenerate energies. Further evidence for inclusion of p bosons emerged from microscopic studies where both the positive parity S-D and negative parity P-F pair structure of the nuclear wavefunction were analyzed [10,11]. The probability of the P pair was found to be comparable to that of the F pair in deformed actinides [11]. Finally, phenomenological studies revealed that using the $spdf$-IBM resulted in an improved description of negative parity states, especially in regions of strong octupole collectivity [12–15]. For example, $E1$ transitions in Ba isotopes could be described well only with the inclusion p bosons [14]. It is important to emphasize that while the quadrupole and octupole collectivities represented by the d and f bosons are with respect to the single particle operators $r^2Y_{2\mu}$ and $r^3Y_{3\mu}$, the dipole collectivity embodied by the p boson is not associated with $r^1Y_{1\mu}$, which corresponds to the spurious center of mass motion. Rather it arises from coherent many-body correlations in the intrinsic wave function under strong quadrupole and octupole fields [11].

Application of the ensuing $spdf$-IBM formalism has been limited in practice due to a number of problems. The first is the excessive number of parameters in the model; the most general $spdf$-IBM Hamiltonian with one- and two-body interactions contains 53 terms. This drastic increase in the number of parameters is accompanied with a reduced set of available data for negative parity states. Thus for practical applications, it is essential to find a much reduced parameter set that still describes the basic features of octupole excitations. This is a physics problem that requires finding a minimal Hamiltonian and relating its parameters to spectra so that an intuitive understanding of the $spdf$-IBM at a level similar to that of the sd-IBM is achieved. In this respect, a mean field analysis of the $spdf$-IBM would be very useful. Such a study has been carried out previously using the SU(3) intrinsic states with a quadrupole-plus-octupole Hamiltonian [16]. However, problems with self-consistency, lack of single-boson energies and enforcement of the SU(3) parameters limits the utility of this study for the above purpose.

A second problem in application of the $spdf$-IBM arises from the diagonalization of the Hamiltonian in the full $spdf$ space, which is too large to carry out without truncation. This is more of a technical nature and can be overcome using angular momentum projected mean field theory [13], which leads to a $1/N$ expansion [17,18]. However, because projection is quite a laborious procedure, a simpler strategy would be to first study the general features of the model using the mean field theory (without projection), and then perform angular momentum projection for the purpose of detailed comparisons with spectra.

Due to their hindered accessibility, data on octupole excitations used to be quite meager compared to the quadrupole ones. This situation has changed dramatically in recent years

with the arrival of the γ-ray arrays. The negative-parity spectra in actinide nuclei Rn, Ra, and Th have been greatly extended using the γ-ray arrays Eurogam and Gammasphere [19–21]. These new data, in turn, provide fresh challenges for collective models, for example, description of the conjectured transition from octupole vibrational to octupole deformed shapes in actinides [22]. Another challenge for the theory is to accommodate the $K^\pi=3^-$ band in the same energy regime ($\sim$1.5 MeV) as the other one-phonon bands. Due to lack of observation, the $K^\pi=3^-$ bands in deformed nuclei had been assumed to lie at much higher energies in previous systematic studies [6–8]. The recent observation of this band at 1571 keV in ^{162}Dy [23] calls for re-examination of these IBM fits to the negative-parity bands in rare earths and actinides.

In this article, we present a general mean field analysis of the $spdf$-IBM that provides an intuitive understanding of the qualitative features of the model. This first step will be followed in future articles by quantitative calculations with angular momentum projection, where detailed description of nuclei with enhanced octupole correlations will be attempted.

II. FORMALISM

A. Hamiltonian

The general Hamiltonian in the $spdf$-IBM contains too many parameters to be useful in practical applications. To come up with a simpler Hamiltonian that still contains the basic physics of the quadrupole-octupole degrees of freedom, we use the sd-IBM as a guide. After years of distillation, a standard form for the sd-IBM Hamiltonian has been reached that contains just the d-boson energy term and the quadrupole interaction

$$H_{sd}=\varepsilon_d\hat{n}_d-\kappa_2\hat{Q}\cdot\hat{Q}. \tag{1}$$

Here $\hat{n}_d$ is number operator for d bosons, and the quadrupole operator,

$$\hat{Q}_\mu=[s^\dagger\tilde{d}+d^\dagger s]^{(2)}_\mu+\chi_d[d^\dagger\tilde{d}]^{(2)}_\mu, \tag{2}$$

is also used in the $E2$ transition operator, i.e., $T(E2)=e_2Q$, where e_2 is the boson effective charge. The tilde on a boson operator b_{lm} denotes $\tilde{b}_{lm}=(-1)^m b_{l-m}$. The Hamiltonian (1) contains all the dynamical symmetry limits of the IBM and describes both spherical and quadrupole-deformed nuclei.

The above consideration suggests that a minimal description of the octupole degree of freedom could be obtained using the f-boson energy term and the octupole interaction. Increasing the strength of the latter, one can induce octupole deformation as in the case of the sd-IBM. Extending this argument to p bosons, we propose the following minimal Hamiltonian for the $spdf$-IBM that has already been used to describe the negative parity states in the actinide region [13,17]

$$H=\varepsilon_d\hat{n}_d+\varepsilon_p\hat{n}_p+\varepsilon_f\hat{n}_f-\kappa_2\hat{Q}\cdot\hat{Q}-\kappa_1\hat{D}\cdot\hat{D}-\kappa_3\hat{O}\cdot\hat{O}, \tag{3}$$

where the quadrupole, dipole, and octupole operators are defined as

$$\begin{aligned}\hat{Q}_\mu&=[s^\dagger\tilde{d}+d^\dagger s]^{(2)}_\mu+\chi_d[d^\dagger\tilde{d}]^{(2)}_\mu\\&\quad+\chi_-\{\chi_{pf}[p^\dagger\tilde{f}+f^\dagger\tilde{p}]^{(2)}_\mu+\chi_p[p^\dagger\tilde{p}]^{(2)}_\mu+\chi_f[f^\dagger\tilde{f}]^{(2)}_\mu\},\\\hat{D}_\mu&=[s^\dagger\tilde{p}+p^\dagger s]^{(1)}_\mu+\chi_1[d^\dagger\tilde{p}+p^\dagger\tilde{d}]^{(1)}_\mu+\chi_1'[d^\dagger\tilde{f}+f^\dagger\tilde{d}]^{(1)}_\mu,\\\hat{O}_\mu&=[s^\dagger\tilde{f}+f^\dagger s]^{(3)}_\mu+\chi_3'[d^\dagger\tilde{p}+p^\dagger\tilde{d}]^{(3)}_\mu+\chi_3[d^\dagger\tilde{f}+f^\dagger\tilde{d}]^{(3)}_\mu.\end{aligned} \tag{4}$$

Compared to the three parameters of the sd-IBM (1), (2), the $spdf$-IBM Hamiltonian (3), (4) contains 14 free parameters (here χ_- is not free but introduced for convenience). Clearly this is still too many, and a further reduction in the number of parameters is desirable. The sd subset of the parameters are well known from previous studies, e.g., in deformed actinides $\kappa_2\sim$20 keV, $\chi_d\sim-0.9$ [0.7 times the SU(3) value], and $\varepsilon_d\sim1.5N\kappa_2$ [24]. Therefore, in the following we concentrate on the other parameters introduced by the pf bosons. There is sufficient data on octupole excitations to determine its coupling strength κ_3 and energy ϵ_f. The situation with respect to the p bosons, however, is more complicated. There are no $K=1^-$ bands that one can clearly identify as dipole excitations. (Recent data in Nd isotopes indicate existence of a second set of $K=0^-$ and 1^- bands at about 2.5 MeV that have been interpreted as dipole excitations [25]. However more work is needed to eliminate alternative explanations and establish the uniqueness of this interpretation.) In the absence of guidance from experiments, it has been a common practice to take the dipole parameters same as the octupole ones, i.e., $\epsilon_p=\epsilon_f$ and $\kappa_1=\kappa_3$. On another extreme, the p boson has been identified with the giant dipole resonance [26], which puts ϵ_p around 15 MeV. In view of these uncertainties, we take a more flexible approach here. Rather than choosing some arbitrary values, we study sensitivity of the $E1$ and other properties to variations in ϵ_p and κ_1 to see if the available data can be used to restrict their range. The only condition we impose in this study is that $\epsilon_p>\epsilon_f$ and $\kappa_1<\kappa_3$, in line with the stronger octupole collectivity.

The remaining χ parameters are very sensitive to interband transitions and are best determined by them. For example, the quoted value of χ_d follows almost uniquely from the $\gamma\rightarrow$ ground $E2$ transitions. Since there are not sufficient data to determine all the χ parameters in this way, they have been chosen more or less arbitrarily in the past with some guidance from the SU(3) limit (see Table I). While the SU(3) limit provides a useful benchmark for quadrupole deformed nuclei, it is not at all clear whether this can be extended to mixed parity systems. In the following sections, we will seek alternative parametrizations for χ which are physically more appealing.

The explicit form of the Hamiltonian (3) is cumbersome for the purpose of calculating the energy surface as it leads to

TABLE I. The χ parameters in the quadrupole, octupole, and dipole operators. $\bar{\chi}$ is obtained by multiplying χ with the C-G coefficient given in the third column. Unless otherwise stated, the parameter values given in the last column are employed in all the calculations.

	χ	SU(3) C-G	$\bar{\chi}$	adapted $\bar{\chi}$
χ_d	$-\sqrt{7}/2$	$-\sqrt{2/7}$	$1/\sqrt{2}$	0.5
χ_{pf}	$-2\sqrt{7}/5$	$-\sqrt{3/7}$	$2\sqrt{3}/5$	$2\sqrt{3}/5$
χ_p	$3\sqrt{3}/5$	$\sqrt{2/3}$	$3\sqrt{2}/5$	$2\sqrt{2}/5$
χ_f	$\sqrt{42}/5$	$2/\sqrt{21}$	$2\sqrt{2}/5$	$3\sqrt{2}/5$
χ_3	$-\sqrt{6/5}$	$-2/\sqrt{15}$	$2\sqrt{2}/5$	$2\sqrt{3}/5$
χ_3'	$2/\sqrt{5}$	$\sqrt{3/5}$	$2\sqrt{3}/5$	$2\sqrt{2}/5$
χ_1	$-2/\sqrt{5}$	$-\sqrt{2/5}$	$2\sqrt{2}/5$	$2\sqrt{2}/5$
χ_1'	$\sqrt{21/5}$	$3/\sqrt{35}$	$3\sqrt{3}/5$	$3\sqrt{3}/5$

a very lengthy expression. For notational convenience and compact results, it will be handy to introduce a generalized boson system b_{lm}, $l=0,1,2,3,\ldots$, with a generic Hamiltonian

$$H=\sum_l \varepsilon_l \hat{n}_l-\sum_k \kappa_k T^{(k)}\cdot T^{(k)}, \tag{5}$$

where the boson number and multipole operators are given by

$$\hat{n}_l=\sum_m b_{lm}^\dagger b_{lm}, \quad T^{(k)}=\sum_{jl} t_{kjl}[b_j^\dagger \tilde{b}_l]^{(k)}. \tag{6}$$

Here the multipole parameters satisfy $t_{kjl}=t_{klj}$ from hermiticity. The correspondence between t_{kjl} and the χ parameters in Eq. (4) follows from a comparison of operators, e.g., $t_{k0l}=1$, $t_{222}=\chi_d$, $t_{112}=\chi_1$, etc. The parity of the multipole terms in Eq. (5) is restricted to $\pi=(-1)^k$, which are physically the most important ones. For $l=1,2,3$ and $k=1,2,3$ the Hamiltonian (5) is equivalent to that of Eq. (3). As in the sd-IBM, we choose the electric transition operators consistent with the Hamiltonian (5), (6), i.e., $T(Ek)=e_k T^{(k)}$.

We also introduce a dimensionless parameter set that reflects the dominance of the quadrupole interaction

$$\eta_l=\epsilon_l/N\kappa_2, \quad \zeta_l=\kappa_k/\kappa_2. \tag{7}$$

This way one can factor out N and κ_2 from the energy expressions, and the latter can be determined from the overall scale of the spectrum. The above parametrization will be particularly useful in discussion of shape-phase transitions and systematic studies of observables because the results will be independent of N and κ_2.

B. Intrinsic state and parity projection

The ground state of a generalized boson system b_{lm}, $l=0,1,2,3,\ldots$ can be written as a boson condensate [27]

$$|N,\mathbf{x}\rangle=\frac{1}{\sqrt{N!}}(b^\dagger)^N|0\rangle, \quad b^\dagger=\sum_{lm} x_{lm}b_{lm}^\dagger, \tag{8}$$

where x_{lm} are the mean fields that are to be associated with various deformations of the system. The condensate (8) contains a mixture of even and odd parity terms and, therefore, does not have a good parity. States with good parity can be obtained using the projection operator

$$P_\pi=\frac{1}{2}(1+\pi\mathcal{P}), \tag{9}$$

where $\pi=\pm 1$ is the parity quantum number and $\mathcal{P}$ is the parity operator. Under $\mathcal{P}$, boson operators transform as

$$\mathcal{P}b_{lm}^\dagger\mathcal{P}=(-1)^l b_{lm}^\dagger, \tag{10}$$

hence $\mathcal{P}$ acting on the condensate (8) gives

$$\mathcal{P}|N,\mathbf{x}\rangle=|N,\mathbf{x}'\rangle, \quad x_{lm}'=(-1)^l x_{lm}. \tag{11}$$

Using Eqs. (9) and (11), we obtain for the parity projection of the condensate (8)

$$P_\pi|N,\mathbf{x}\rangle=\frac{1}{2\sqrt{N!}}\left[\left(\sum_{lm} x_{lm}b_{lm}^\dagger\right)^N+\pi\left(\sum_{lm} x_{lm}'b_{lm}^\dagger\right)^N\right]|0\rangle. \tag{12}$$

Binomial expanding the even and odd l parts in Eq. (12), it is easy to see that for $\pi=+1$, it has an even number of odd-parity bosons, and for $\pi=-1$, it has an odd number of odd-parity bosons. Note that while the condensate (8) is normalized, this is lost after parity projection. Using $P_\pi^2=P_\pi$, the normalization of the projected state (12) is given by

$$\mathcal{N}_\pi=\langle N,\mathbf{x}|P_\pi|N,\mathbf{x}\rangle=\frac{1}{2}(\mathbf{x}\cdot\mathbf{x})^N(1+\pi r^N), \quad r=\mathbf{x}\cdot\mathbf{x}'/\mathbf{x}\cdot\mathbf{x}. \tag{13}$$

Here r gives a measure of the mixing between the even- and odd-parity bosons. For $r=1$, the ground state corresponds to a condensate of the even-parity bosons only. With decreasing r, mixture of the odd-parity bosons in the condensate increases, becoming an equal mixture at $r=0$. With further reduction in r, the odd-parity bosons start dominating the condensate, reaching the opposite limit of a condensate of the odd-parity bosons at $r=-1$. Thus for weakly coupled octupole vibrations $r\approx 1$, and the limit $r\to 0$ corresponds to the onset of stable octupole deformation.

C. Energy surface and axial symmetry

The energy surface of the Hamiltonian (5) with parity projection is given by

$$E_\pi(\mathbf{x})=\frac{1}{\mathcal{N}_\pi}\langle N,\mathbf{x}|HP_\pi|N,\mathbf{x}\rangle$$
$$=\frac{1}{2\mathcal{N}_\pi}[\langle N,\mathbf{x}|H|N,\mathbf{x}\rangle+\pi\langle N,\mathbf{x}|H|N,\mathbf{x}'\rangle]. \tag{14}$$

The matrix elements in Eq. (14) can be evaluated using boson calculus, yielding

$$E_\pi(\mathbf{x}) = \frac{N^2\kappa_2}{(1+\pi r^N)(\mathbf{x}\cdot\mathbf{x})^2}\Bigg\{(\mathbf{x}\cdot\mathbf{x})\sum_{lm}\eta_l|x_{lm}|^2 \times[1+\pi r^{N-1}(-1)^l] - \sum_{k\mu}\zeta_k[|A_{k\mu}|^2+\pi r^{N-2}|A'_{k\mu}|^2]\Bigg\}, \quad (15)$$

where we have used the dimensionless parameters introduced in Eq. (7). The quadratic forms $A_{k\mu}$ in Eq. (15) are defined by

$$A_{k\mu} = \sum_{jmln}\langle jmln|k\mu\rangle(-1)^n t_{kjl}x^*_{jm}x_{l-n}, \quad (16)$$

and $A'_{k\mu}=A_{k\mu}(\mathbf{x},\mathbf{x}')$. In deriving Eq. (15), we have ignored the $1/N$ correction terms in the two-body part in the spirit of the large N interpretation of the energy surface. This is equivalent to using the normal ordered forms of the multipole interactions. The result without parity projection can be obtained from Eq. (15) by ignoring the parity projected terms, i.e., by setting $\pi=0$.

Finding the minimum of the energy surface (15) for a general condensate is a rather difficult problem. In the $spdf$-IBM, there are $\Sigma_l(2l+1)=16$ mean fields which could, in general, be complex. In order to make progress, it is essential to reduce the number of mean fields in the variational problem using symmetry and physics arguments. To start with, we can set $x_{00}=1$ from the normalization condition. Unlike the quadrupole deformation, there are no space symmetries in the intrinsic frame for a mixed parity system. The only other symmetry one can invoke is time reversal, which gives $x_{lm}=(-1)^m x^*_{l-m}$. This reduces the number of independent mean fields by half to three real x_{l0} and six complex x_{lm} with $m>0$. In fact, in all our test runs the real and complex mean fields led to the same result, consistent with the observation [28] that only real mean fields are needed in the intrinsic frame.

From experimental observations, axial symmetry appears to be maintained to a good approximation in the ground states of deformed nuclei. In the sd-IBM, axial symmetry is well known to be preserved [27], and we expect that this will also hold true in realistic cases of the $spdf$-IBM. We have checked this conjecture using the explicit form of the Hamiltonian (3). The energy surface of the Hamiltonian (3) can be worked out from the expressions given in Eqs. (15) and (16) by inserting the appropriate Clebsch-Gordan coefficients. For a given parameter set, the absolute minimum of the energy surface is determined numerically using the simplex method, and the nature of the solutions (i.e., whether axially symmetric or not) is noted. We consider variations in three parameters that are expected to play a role in octupole deformation, namely, κ_3, χ_3, and χ_-. The other χ values are taken from Table I and for the rest we use $\eta_1=15$, $\eta_2=1.5$, $\eta_3=3$, $\zeta_1=0.1$. The results of this study covering a wide range of the parameter values are summarized in Fig. 1. The lines correspond to different values of $\zeta_3=\kappa_3/\kappa_2$, which is varied from 0.1 (top line) to 1.0 (bottom line) in steps of 0.3. The regions below the lines correspond to parameter values leading axially symmetric mean fields. Thus, as long as χ_3 is negative, the system remains axially symmetric, regardless of the other parameters. Notice that with increasing ζ_3 the lines quickly converge towards $\chi_3=0$ line, and χ_- has a rather marginal effect on the results. As seen from Table I, a negative χ_3 value naturally occurs in the SU(3) limit. In the following, we will stick to the negative χ_3 values and present more reasons in the next sections why this choice is more physical as well as being more convenient.

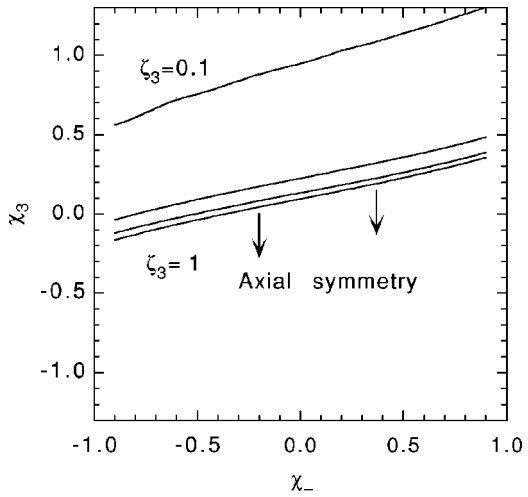

FIG. 1. Regions of axial symmetry in the $spdf$-IBM parameter space. The lines, from top to bottom, correspond to fixed octupole strengths with $\zeta_3=\kappa_3/\kappa_2=0.1$, 0.4, 0.7, and 1.0, respectively. For parameter values below each line the boson system remains axially symmetric while above the line it becomes nonaxial.

While our focus in this work is on axially symmetric systems, Fig. 1 also indicates that nonaxial shapes can be easily obtained in the $spdf$-IBM using the basic Hamiltonian (3) with positive χ_3 values. This in contrast to the sd-IBM where introduction of higher order interactions is necessary in order to induce nonaxial shapes.

The proof of axial symmetry brings in an enormous simplification to the mean field problem, which we exploit in the following to get a better understanding of the model parameters. The ground state of the boson system is still given by the condensate (8) but with the sum restricted to the $m=0$ terms only. Henceforth, we will suppress the 0 subscript for convenience and denote the mean fields by x_l. When x_0 is set to 1 from normalization, it is customary to denote the remaining mean fields by $\beta_l\equiv x_l$. We follow this practice in this work. It should be noted that the IBM deformation parameters β_l are different from their geometrical model counterparts. Since they represent only the deformation associated with the valence nucleons, they are typically a factor of 3–4 larger than the liquid drop values [27].

D. Eigenmode conditions

For axially symmetric systems, the variational problem for a given multipole interaction $H_k=-\kappa_k T^{(k)}\cdot T^{(k)}$ is

equivalent to the eigenmode condition for the operator $T^{(k)}$. Hence, the effect of a particular multipole interaction on the intrinsic state $b^\dagger$, which is not so easy to surmise from the energy surface (15), can be simply obtained from the eigenmode condition defined by

$$[T_0^{(k)}, b^\dagger] = \lambda_k b^\dagger. \tag{17}$$

Using Eq. (6) in the commutator one obtains an eigenvalue equation for the mean fields

$$\sum_j \bar{t}_{kjl} x_j = \lambda_k x_l. \tag{18}$$

The eigenvalues λ_k correspond to the extremum values of the energy surface, given by $\langle H_k \rangle = -N^2 \lambda_k^2$ to leading order in N. Here (and on the χ parameters, see Table I) bar denotes Clebsch-Gordan weighted parameters, that is,

$$\bar{t}_{kjl} = \langle j0l0|k0\rangle t_{kjl}. \tag{19}$$

We consider the eigenmode condition for each of the multipole operators in Eq. (4) to see their effect on the condensate. For the quadrupole operator, Eq. (18) can be written explicitly as

$$\begin{pmatrix} 0 & 1 & 0 & 0 \\ 1 & \bar{\chi}_d & 0 & 0 \\ 0 & 0 & \bar{\chi}_p & \bar{\chi}_{pf} \\ 0 & 0 & \bar{\chi}_{pf} & \bar{\chi}_f \end{pmatrix} \begin{pmatrix} x_0 \\ x_2 \\ x_1 \\ x_3 \end{pmatrix} = \lambda_2 \begin{pmatrix} x_0 \\ x_2 \\ x_1 \\ x_3 \end{pmatrix}, \tag{20}$$

where we have set $\chi_- = 1$ for simplicity and grouped the even and odd parity mean fields separately for clarity of demonstration. The block diagonal form of Eq. (20) shows that the $Q \cdot Q$ interaction does not mix the positive and negative parity bosons. In general, there are two solutions of Eq. (20), one associated with the positive parity mean fields and the other with the negative parity ones

$$\lambda_{2+} = \frac{1}{2}[\bar{\chi}_d \pm \sqrt{\bar{\chi}_d^2 + 4}], \quad \mathbf{x}_+ = (1, \lambda_{2+}, 0, 0),$$

$$\lambda_{2-} = \frac{1}{2}[\bar{\chi}_p + \bar{\chi}_f \pm \sqrt{(\bar{\chi}_p - \bar{\chi}_f)^2 + 4\bar{\chi}_{pf}^2}],$$

$$\mathbf{x}_- = (0, 0, 1, (\lambda_{2-} - \bar{\chi}_p)/\bar{\chi}_{pf}), \tag{21}$$

where $\mathbf{x} = (x_0, x_2, x_1, x_3)$ as above. For a prolate shape, that we assume in this work, the + signs in Eq. (21) minimize the energy and maximize the quadrupole moment (see below). When $\lambda_{2+} > \lambda_{2-}$, the ground state is a condensate of sd bosons, and when $\lambda_{2+} < \lambda_{2-}$ it is a condensate of pf bosons. The case $\lambda_{2+} = \lambda_{2-}$ corresponds to the critical point in between. We have chosen the relative scale factor in the pf sector of the SU(3) quadrupole parameters (Table I) such that $\lambda_{2+} = \lambda_{2-} = \sqrt{2}$ in this limit. Then, an arbitrary combination of the solutions $\mathbf{x}_+ = (1, \sqrt{2}, 0, 0)$ and $\mathbf{x}_- = (0, 0, \sqrt{3}, \sqrt{2})$ satisfies Eq. (20). Note that contrary to the expected dominance of octupole over dipole collectivity, the SU(3) values lead to $x_1 > x_3$. A more realistic parametrization that we adapt here is obtained by simply interchanging the values of $\bar{\chi}_p$ and $\bar{\chi}_f$ in Table I, which gives the same λ_{2-} but with the mean fields interchanged, that is $\mathbf{x}_- = (0, 0, \sqrt{2}, \sqrt{3})$. In general, one can always set $\chi_- = \lambda_{2+}/\lambda_{2-}$ in the quadrupole operator (4) so that sd and pf sectors simultaneously satisfy Eq. (20). In realistic parametrizations, however, $Q \cdot Q$ interaction alone should lead to a quadrupole deformation only. For the quadrupole parameters used in this work (Table I), this imposes the condition $|\chi_-| < 0.9$.

Next consider the eigenmode condition for the octupole operator, which leads to the eigenvalue equation

$$\begin{pmatrix} 0 & 0 & 0 & 1 \\ 0 & 0 & \bar{\chi}_3' & \bar{\chi}_3 \\ 0 & \bar{\chi}_3' & 0 & 0 \\ 1 & \bar{\chi}_3 & 0 & 0 \end{pmatrix} \begin{pmatrix} x_0 \\ x_2 \\ x_1 \\ x_3 \end{pmatrix} = \lambda_3 \begin{pmatrix} x_0 \\ x_2 \\ x_1 \\ x_3 \end{pmatrix}. \tag{22}$$

Notice that the structure of Eq. (22) is completely opposite to that of Eq. (20), with zero block diagonal terms and nonzero off diagonal terms. This leads to a mixing of positive and negative parity mean fields in the intrinsic state which was not possible with a $Q \cdot Q$ interaction. The discriminant of Eq. (22) is quadratic in λ_3^2

$$\lambda_3^4 - (\bar{\chi}_3^2 + \bar{\chi}_3'^2 + 1)\lambda_3^2 + \bar{\chi}_3'^2 = 0, \tag{23}$$

which has the solutions

$$\lambda_3^2 = \frac{1}{2}[\bar{\chi}_3^2 + \bar{\chi}_3'^2 + 1 \pm \sqrt{(\bar{\chi}_3^2 + \bar{\chi}_3'^2 + 1)^2 - 4\bar{\chi}_3'^2}],$$

$$\mathbf{x} = \left(1, \frac{\lambda_3^2 - 1}{\bar{\chi}_3}, \frac{\bar{\chi}_3'(\lambda_3^2 - 1)}{\bar{\chi}_3 \lambda_3}, \lambda_3\right). \tag{24}$$

Using the SU(3) values from Table I gives $\lambda_3^2 = (9 + \sqrt{33})/10 = 1.474$ and $\mathbf{x} = (1, 0.839, 0.478, 1.214)$. Thus the octupole interaction leads to an enhanced octupole deformation as expected. Unlike in other cases, the SU(3) tensor operator here results in irrational eigenvalues, and further the pd coupling is stronger than the fd coupling ($\bar{\chi}_3' > \bar{\chi}_3$). In the realistic set (Table I), we interchange these two values which sorts out both of these problems, giving $\lambda_3^2 = 8/5$ and $\mathbf{x} = (1, \sqrt{3}/2, \sqrt{3/20}, \sqrt{8/5})$. Note that for $\chi_3 < 0$ ($\bar{\chi}_3 > 0$), the mean fields in Eq. (24) are coherent with those obtained from the quadrupole interaction, which reinforces the axial symmetry in the combined Hamiltonian. Positive χ_3 values, on the other hand, lead to conflicting signs in the mean fields, giving rise to the nonaxial shapes.

Finally, the eigenmode condition for the dipole operator gives

$$\begin{pmatrix} 0 & 0 & 1 & 0 \\ 0 & 0 & \overline{\chi}_1 & \overline{\chi}'_1 \\ 1 & \overline{\chi}_1 & 0 & 0 \\ 0 & \overline{\chi}'_1 & 0 & 0 \end{pmatrix} \begin{pmatrix} x_0 \\ x_2 \\ x_1 \\ x_3 \end{pmatrix} = \lambda_1 \begin{pmatrix} x_0 \\ x_2 \\ x_1 \\ x_3 \end{pmatrix}. \tag{25}$$

The structure of Eq. (25) is very similar to that of Eq. (22), and one obtains the same equation for λ_1 as for λ_3 in Eq. (23) with all the subscripts 3 replaced by 1. The mean field solutions are thus given by

$$\lambda_1^2 = \frac{1}{2}[\overline{\chi}_1^2 + \overline{\chi}_1'^2 + 1 \pm \sqrt{(\overline{\chi}_1^2 + \overline{\chi}_1'^2 + 1)^2 - 4\overline{\chi}_1'^2}],$$

$$\mathbf{x} = \left(1, \frac{\lambda_1^2 - 1}{\overline{\chi}_1}, \lambda_1, \frac{\overline{\chi}'_1(\lambda_1^2 - 1)}{\overline{\chi}_1 \lambda_1}\right). \tag{26}$$

Substituting the SU(3) values above, we obtain $\lambda_1^2 = 9/5$ and $\mathbf{x} = (1, \sqrt{2}, 3/\sqrt{5}, \sqrt{6/5})$. Compared to the octupole interaction, the dipole interaction leads to a more even distribution among the various deformations.

The mean field solutions obtained from the eigenmode conditions clearly demonstrate the basic incompatibility among the various multipole interactions. For example, in the quadrupole SU(3) solutions, $x_2 > x_0$ and $x_1 > x_3$, which is opposite to that obtained in the octupole SU(3) case. Thus mixing of the two quadrupole solutions $\mathbf{x}_+$ and $\mathbf{x}_-$ in a quadrupole-plus-octupole Hamiltonian, as is done in Ref. [16], cannot yield a consistent solution for the mean fields. While independent variation of three mean fields is considerably more complicated to handle analytically, this can be easily achieved using numerical techniques.

E. Multipole moments

In the intrinsic frame, the static moment associated with a multipole operator $T^{(k)}$ is given by

$$T_{k0} = \frac{\langle N, \mathbf{x} | T_0^{(k)} | N, \mathbf{x} \rangle}{\langle N, \mathbf{x} | N, \mathbf{x} \rangle} = N \sum_{jl} \overline{t}_{kjl} x_j x_l. \tag{27}$$

In terms of the mean fields $\mathbf{x} = (1, \beta_1, \beta_2, \beta_3)$, the quadrupole, octupole and dipole moments have the particular forms

$$Q_0 = \frac{N}{\mathbf{x}\cdot\mathbf{x}}[2\beta_2 + \overline{\chi}_d \beta_2^2 + \chi_- (2\overline{\chi}_{pf} \beta_1 \beta_3 + \overline{\chi}_p \beta_1^2 + \overline{\chi}_f \beta_3^2)],$$

$$O_0 = \frac{2N}{\mathbf{x}\cdot\mathbf{x}}[\beta_3 + \overline{\chi}_3 \beta_2 \beta_3 + \overline{\chi}'_3 \beta_1 \beta_2],$$

$$D_0 = \frac{2N}{\mathbf{x}\cdot\mathbf{x}}[\beta_1 + \overline{\chi}_1 \beta_1 \beta_2 + \overline{\chi}'_1 \beta_2 \beta_3]. \tag{28}$$

There is some arbitrariness in the choice of phases in the SU(3) limit. We have fixed the signs of the parameters in Table I such that all the terms in Eq. (28) add coherently to yield the maximum moments. For example, in most previous work the opposite sign for χ_{pf} was used. While this has no effect on the quadrupole moment itself, the resulting mean fields lead to cancellations in the octupole moment, reducing the effectiveness of the octupole interaction. The choice of negative χ_3 ($\overline{\chi}_3 > 0$), required for axial symmetry, is also seen to maximize the octupole moment.

The static moment associated with a particular multipole interaction $T^{(k)} \cdot T^{(k)}$ follows trivially from the eigenmode condition (18) as

$$T_{k0} = N\lambda_k = N\beta_k, \tag{29}$$

where $\beta_k = \lambda_k$ used in the last step follows from Eqs. (21), (24), (26). Thus the static moments are simply proportional to the corresponding deformation parameter when the Hamiltonian is restricted to a certain multipolarity.

With parity projection, the multipole matrix element in Eq. (27) becomes

$$\begin{aligned} T_{k0}^{\pi,\pi'} &= [\mathcal{N}_\pi \mathcal{N}_{\pi'}]^{-1/2} \langle N, \mathbf{x} | P_\pi T_0^{(k)} P_{\pi'} | N, \mathbf{x} \rangle \\ &= \frac{[1 + (-1)^k \pi\pi']}{4[\mathcal{N}_\pi \mathcal{N}_{\pi'}]^{1/2}} [\langle N, \mathbf{x} | T_0^{(k)} | N, \mathbf{x} \rangle \\ &\quad + \pi \langle N, \mathbf{x} | T_0^{(k)} | N, \mathbf{x}' \rangle]. \end{aligned} \tag{30}$$

For $\pi = \pi'$, Eq. (30) gives essentially the same result as Eq. (27) for even multipoles, but it vanishes for odd ones. To discuss the odd-multipole moments, one can either use Eq. (27) or introduce transition moments by

$$T_{k0}^{+-} = [1 - r^{2N}]^{-1/2} T_{k0}, \tag{31}$$

where T_{k0} are given in Eq. (28). When there is a substantial mixture of odd-parity bosons in the ground state, $r \ll 1$, and the two results are seen to merge. We will consider both options in discussing octupole moments.

III. SHAPE-PHASE TRANSITIONS

Shape-phase transitions in the sd-IBM has been well studied in earlier works [27,29]. For comparison purposes we summarize the results for spherical to quadrupole-deformed shape transition here. The energy surface of the Hamiltonian (1) is given by

$$E_{sd}(\beta_2) = N^2 \kappa_2 \left[\frac{\eta_2 \beta_2^2}{1 + \beta_2^2} - \left(\frac{2\beta_2 + \overline{\chi}_d \beta_2^2}{1 + \beta_2^2} \right)^2 \right], \tag{32}$$

where η_2 was introduced in Eq. (7). Variation of Eq. (32) with respect to β_2 gives a fourth degree polynomial equation

$$\beta_2[\eta_2(1 + \beta_2^2) - 2(2 + \overline{\chi}_d \beta_2)(1 + \overline{\chi}_d \beta_2 - \beta_2^2)] = 0. \tag{33}$$

The critical point for the phase transition from spherical to quadrupole-deformed shape is given by

$$\eta_2 = 4 + \overline{\chi}_d^2, \quad \text{or} \quad \kappa_2 = \frac{\epsilon_d}{N(4 + \overline{\chi}_d^2)}. \tag{34}$$

At the critical point, the spherical ($\beta_2=0$) and deformed ($\beta_2=\bar{\chi}_d/2$) minima coexist, both having the energy $E=0$. Note that with angular momentum projection, one obtains the same leading order expression for the energy surface as in Eq. (32) [30]. Thus restoration of the broken rotational invariance causes only a small change of order $1/N$ in the shape-phase diagram.

As shown in Ref. [31], shape-phase transitions in the sf-IBM are very similar to those in the sd-IBM if one ignores parity projection. For a Hamiltonian consisting of one-body energy and octupole interaction, the critical point for the onset of octupole deformation occurs at $\kappa_3=\epsilon_f/4N$, which is the same as Eq. (34) if we set $\chi_d=0$ (the difference is due to the lack of a $f^\dagger\tilde{f}$ term in the octupole operator because it has positive parity). This well-known picture for shape-phase transitions, however, completely changes after parity projection (PP), with the critical point moving to $\kappa_3=0$ [31]. In the following, we generalize this result to the sdf- and $spdf$-IBM. That is, we show that the onset of the octupole deformation is immediate in the presence of any octupole strength ($\kappa_3\neq 0$) regardless of whether the system is quadrupole deformed or not. For this purpose we use the axially symmetric version of the energy surface (15), which can be written as

$$E_\pi(\beta_1,\beta_2,\beta_3) = \frac{N^2\kappa_2}{(1+\pi r^N)(\mathbf{x}\cdot\mathbf{x})^2}\left\{(\mathbf{x}\cdot\mathbf{x})\sum_{l=1}^{3}\eta_l\beta_l^2[1+\pi r^{N-1}(-1)^l] - (A_{20}^2+\pi r^{N-2}A_{20}'^2)-\zeta_1 A_{10}^2-\zeta_3 A_{30}^2\right\}, \tag{35}$$

where $\mathbf{x}=(1,\beta_1,\beta_2,\beta_3)$ and the dimensionless parameters introduced in Eq. (7) are employed. The quadratic forms in Eq. (35) have the explicit forms

$$A_{20}=2\beta_2+\bar{\chi}_d\beta_2^2+\chi_-(2\bar{\chi}_{pf}\beta_1\beta_3+\bar{\chi}_p\beta_1^2+\bar{\chi}_f\beta_3^2),$$

$$A_{10}=2\beta_1+2\bar{\chi}_1\beta_1\beta_2+2\bar{\chi}_1'\beta_2\beta_3,$$

$$A_{30}=2\beta_3+2\bar{\chi}_3'\beta_1\beta_2+2\bar{\chi}_3\beta_2\beta_3, \tag{36}$$

with $A_{20}'=A_{20}(-\chi_-)$. Note that $A_{10}'=A_{30}'=0$ because the hermitian conjugate of each term contributes with an opposite sign in odd-parity operators.

A. *sdf*-IBM

We first consider the sdf-IBM both because of its relevance (p boson is presumably weakly coupled) and also for convenience (analytic solutions are still possible with two mean fields but not with three). The energy surface in the sdf-IBM follows from Eq. (35) by setting $\beta_1=\zeta_1=0$ and $\chi_-=1$. Without PP ($\pi=0$), this energy surface further simplifies to

$$E_{sdf}(\beta_2,\beta_3)=\frac{N^2\kappa_2}{(1+\beta_2^2+\beta_3^2)^2}[(1+\beta_2^2+\beta_3^2)(\eta_2\beta_2^2+\eta_3\beta_3^2) - (2\beta_2+\bar{\chi}_d\beta_2^2+\bar{\chi}_f\beta_3^2)^2-4\zeta_3(\beta_3+\bar{\chi}_3\beta_2\beta_3)^2]. \tag{37}$$

Setting the derivatives of E_{sdf} with respect to β_2 and β_3 to zero, we find for the extremum conditions

$$\beta_2(1+\beta_2^2+\beta_3^2)[\eta_2+(\eta_2-\eta_3)\beta_3^2]-4\zeta_3\beta_3^2(1+\bar{\chi}_3\beta_2) \times[\bar{\chi}_3(1-\beta_2^2+\beta_3^2)-2\beta_2]-2(2\beta_2+\bar{\chi}_d\beta_2^2+\bar{\chi}_f\beta_3^2) \times[(1+\bar{\chi}_d\beta_2)(1+\beta_3^2)-\beta_2(\beta_2+\bar{\chi}_f\beta_3^2)]=0, \tag{38}$$

$$\beta_3\{(1+\beta_2^2+\beta_3^2)[\eta_3+(\eta_3-\eta_2)\beta_2^2]-4\zeta_3(1+\bar{\chi}_3\beta_2)^2 \times(1+\beta_2^2-\beta_3^2)+2(2\beta_2+\bar{\chi}_d\beta_2^2+\bar{\chi}_f\beta_3^2) \times[2\beta_2+\bar{\chi}_d\beta_2^2-\bar{\chi}_f(1+\beta_2^2)]\}=0. \tag{39}$$

Note that Eq. (39) has the form $\beta_3(C_2\beta_3^2-C_0)=0$. Thus it has either the trivial solution $\beta_3=0$, in which case the energy minima correspond to those of E_{sd} as discussed above, or $\beta_3^2=C_0/C_2$, which could lead to an octupole deformed minimum. Substituting this value of β_3^2 back in Eq. (38) leads to an 8th degree polynomial equation in β_2, which we will not pursue here. What we are really interested in is finding the critical point for the onset of octupole deformation, which can be determined without explicitly solving for β_2 and β_3. At the critical point, the octupole deformed solution coexists with the vibrational one ($\beta_3=0$) with a vanishingly small β_3. Thus the condition for criticality is simply given by $C_0=0$, which can be written from Eq. (39) as

$$C_0=(1+\beta_2^2)[\eta_2\beta_2^2-\eta_3(1+\beta_2^2)+4\zeta_3(1+\bar{\chi}_3\beta_2)^2] -2(2\beta_2+\bar{\chi}_d\beta_2^2)[2\beta_2+\bar{\chi}_d\beta_2^2-\bar{\chi}_f(1+\beta_2^2)]=0. \tag{40}$$

Using Eq. (33) in (40) to eliminate the η_2 term and reverting back to the original parameters, this condition can be cast into a physically more transparent form

$$\kappa_3=\frac{1}{(1+\bar{\chi}_3\beta_2)^2}\left[\frac{\epsilon_f}{4N}(1+\beta_2^2)+\frac{\kappa_2}{2}(\beta_2-\bar{\chi}_f)(2\beta_2+\bar{\chi}_d\beta_2^2)\right]. \tag{41}$$

For $\beta_2=0$, the condition (41) reduces to $\kappa_3=\epsilon_f/4N$, consistent with the sf-IBM result. For realistic values of parameters ($\beta_2\approx 1$), the presence of the quadrupole deformation is seen to shift the critical κ_3 to larger values, thus retarding the onset of octupole deformation further compared to the spherical case.

Before proceeding with the parity projected case, we remark that the same result can also be obtained by expanding the energy surface around $\beta_3=0$ and examining the coefficient of the β_3^2 term. This method will be useful in compli-

cated cases where manipulation of the extremum equations is substantially more difficult. Expansion of E_{sdf} in Eq. (37) gives

$$E_{sdf}(\beta_2,\beta_3)=E_{sd}(\beta_2)-N^2\kappa_2 C_0(1+\beta_2^2)^{-3}\beta_3^2+\cdots, \tag{42}$$

where E_{sd} and C_0 are defined in Eqs. (32) and (40), respectively. We see from Eq. (42) that for $C_0<0$ the energy surface is stable at $\beta_3=0$ and there is no octupole deformation (in the above discussion, this corresponds to the second β_3 solution becoming imaginary). Conversely, for $C_0>0$ the energy surface becomes unstable at $\beta_3=0$ and the system becomes octupole deformed. Clearly $C_0=0$ corresponds to the critical point, leading to the characteristic flat-bottomed energy surface in the β_3 direction.

We next consider the effect of PP on the octupole shape-phase transition. The sdf-IBM energy surface with $\pi=+1$ is given by

$$\begin{aligned} E_{+sdf}(\beta_2,\beta_3)=\frac{N^2\kappa_2}{(1+r^N)(1+\beta_2^2+\beta_3^2)^2}\Big\{&(1+\beta_2^2+\beta_3^2)\\ &\times\sum_{l=2}^{3}\eta_l\beta_l^2[1+r^{N-1}(-1)^l]\\ &-(2\beta_2+\overline{\chi}_d\beta_2^2+\overline{\chi}_f\beta_3^2)^2-r^{N-2}(2\beta_2\\ &+\overline{\chi}_d\beta_2^2-\overline{\chi}_f\beta_3^2)^2-4\zeta_3(\beta_3+\overline{\chi}_3\beta_2\beta_3)^2\Big\}. \end{aligned} \tag{43}$$

As the extremum conditions lead to unwieldy expressions, we follow the second method here to find the critical point and expand the energy surface (43) around $\beta_3=0$. After some algebra, we obtain to leading order in β_3^2

$$E_{+sdf}(\beta_2,\beta_3)=E_{sd}(\beta_2)-2N^2\kappa_3(1+\beta_2^2)^{-2}(1+\overline{\chi}_3\beta_2)^2\beta_3^2+\cdots. \tag{44}$$

Comparing Eq. (44) with Eq. (42), we see that contributions from the positive parity operators to the β_3^2 term have all disappeared after PP, leaving behind only the octupole term. Obviously, for any finite octupole strength $\kappa_3>0$, the system has an octupole deformation. The inescapable conclusion is that PP has a drastic effect on the onset of octupole deformation moving the required octupole strength from a finite value to zero, that is, the critical point occurs at $\kappa_3=0$ after PP.

Because this is a somewhat surprising result whose derivation from Eq. (43) is not so transparent, we expand on it a little. Comparing Eq. (37) with Eq. (43), it is seen that the matrix elements (m.e.) of the positive parity operators have all acquired a π-dependent term after projection whereas such a term is missing in the m.e. of the negative parity octupole operator. Disappearance of the m.e. of the positive parity operators from the β_3^2 term in Eq. (44) is precisely due to the cancellation between the unprojected and π-dependent terms. A more direct way to see the effect of PP is to expand the sdf-boson condensate

$$\begin{aligned}(s^\dagger+\beta_2 d_0^\dagger+\beta_3 f_0^\dagger)^N&=(s^\dagger+\beta_2 d_0^\dagger)^N+N(s^\dagger+\beta_2 d_0^\dagger)^{N-1}\beta_3 f_0^\dagger\\ &\quad+(1/2)N(N-1)(s^\dagger+\beta_2 d_0^\dagger)^{N-2}(\beta_3 f_0^\dagger)^2+\cdots, \end{aligned} \tag{45}$$

and look at the overlaps of various terms. Denoting the states in the expansion by their f boson number n_f, the leading contribution to the one-body terms comes from the (1-1) m.e. (i.e. $\langle 1|\hat{n}_f|1\rangle$), which goes as β_3^2. However, after PP, odd n_f terms are projected out, so the leading term has to come from the (2-2) m.e., which goes as β_3^4. A similar argument applies to the quadrupole m.e. In contrast, the leading (equal) contributions to the octupole term come from the (1-1) and (0-2 + 2-0) m.e., and PP blocks only the first one, leaving the second one intact [which explains the 1/2 reduction in the κ_3 term in Eq. (44) compared to Eq. (42)]. Thus the net effect of PP is to lift the obstruction of the one-body and quadrupole interaction terms in the Hamiltonian against the formation of an octupole deformed system. In the absence such resistance, even the slightest octupole perturbation is sufficient to deform the system.

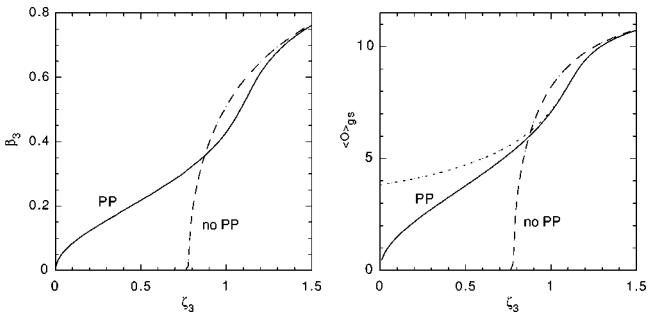

FIG. 2. Shape-phase diagrams depicting the onset of octupole deformation in the presence of quadrupole deformation with PP (solid line) and without PP (dashed line). The β_3 values corresponding to the absolute minimum of the energy surfaces Eqs. (37) and (43) are plotted against $\zeta_3=\kappa_3/\kappa_2$ on the left. The corresponding octupole moments calculated from Eq. (28), together with the transition moment from Eq. (31) (dotted line), are shown on the right.

We summarize the results of this section with a shape-phase diagram shown in Fig. 2. On the left, the β_3 values obtained from the absolute minimum of the energy surface with and without PP are plotted against $\zeta_3=\kappa_3/\kappa_2$, while the figure on the right shows the corresponding octupole moments obtained from Eq. (28). Here the χ parameters are taken from Table I, and the others are; $\eta_2=1.5$, $\eta_3=3$. Without PP, a sharp shape-phase transition to octupole deformation is seen to occur at the critical point given by Eq. (41). After PP, the critical point moves to $\kappa_3=0$ and the sharp transition is replaced by a smoothly varying curve. Note that there is a very close correlation between the β_3 values and the static octupole moments. Thus the exact proportionality found between the two quantities for a particular multipole Hamiltonian [see Eq. (29)] is more or less preserved in the

more general case, confirming the interpretation of the β_3 mean field as the octupole deformation parameter. The transition octupole moment (dotted line), on the other hand, deviates from the static one for small β_3 and does not provide a reliable measure of the octupole deformation in this region.

We remark that the concept of mean field is useful only when the symmetries broken in the intrinsic frame do not have an appreciable effect on the calculated values of physical quantities. Breaking of the rotational symmetry is such an example. As pointed out earlier, one obtains the same energy surface to leading order in N with and without angular momentum projection. Thus the mean field results obtained in the intrinsic frame are accurate to order $1/N$. As demonstrated here, in mixed parity systems the mean field results without PP are dramatically different from those with PP. Therefore mean field studies of mixed parity systems should be carried out with PP, otherwise one is likely to obtain erroneous results especially at small octupole deformations.

B. *spdf*-IBM

The previous result on the onset of octupole deformation can be extended to the $spdf$-IBM in a straightforward manner, though the algebra is considerably more involved. The energy surface in the $spdf$-IBM without PP is obtained from Eq. (35) by setting $\pi=0$. Because the analysis of the extremum conditions is quite complicated, we directly expand this energy surface for small β_1 and β_3, keeping only the quadratic terms

$$\begin{aligned}
&E_{spdf}(\beta_1,\beta_2,\beta_3)\\
&\quad=E_{sd}(\beta_2)+N^2\kappa_2(1+\beta_2^2)^{-2}([\eta_1(1+\beta_2^2)-\eta_2\beta_2^2\\
&\qquad+2(2\beta_2+\overline{\chi}_d\beta_2^2)^2(1+\beta_2^2)^{-1}-2\chi_-(2\beta_2+\overline{\chi}_d\beta_2^2)\overline{\chi}_p\\
&\qquad-4\zeta_1(1+\overline{\chi}_1\beta_2)^2-4\zeta_3(\overline{\chi}_3'\beta_2)^2]\beta_1^2\\
&\qquad-\{2\chi_-(2\beta_2+\overline{\chi}_d\beta_2^2)\overline{\chi}_{pf}+4[\zeta_1(1+\overline{\chi}_1\beta_2)\overline{\chi}_1'\\
&\qquad+\zeta_3(1+\overline{\chi}_3\beta_2)\overline{\chi}_3']\beta_2\}2\beta_1\beta_3+[\eta_3(1+\beta_2^2)-\eta_2\beta_2^2\\
&\qquad+2(2\beta_2+\overline{\chi}_d\beta_2^2)^2(1+\beta_2^2)^{-1}-2\chi_-(2\beta_2+\overline{\chi}_d\beta_2^2)\overline{\chi}_f\\
&\qquad-4\zeta_1(\overline{\chi}_1'\beta_2)^2-4\zeta_3(1+\overline{\chi}_3\beta_2)^2]\beta_3^2+\cdots).
\end{aligned}\tag{46}$$

In order to facilitate the discussion of shape-phase transition, we rewrite this energy surface as

$$E_{spdf}(\beta_1,\beta_2,\beta_3)=E_{sd}(\beta_2)+A\beta_1^2+2B\beta_1\beta_3+C\beta_3^2+\cdots,\tag{47}$$

where the coefficients A, B, and C can be read off from Eq. (46). The behavior of the quadratic form (47) is determined by the sign of its discriminant.

(i) $B^2-AC<0$: the energy surface has a bowl shape in the β_1-β_3 plane. When the quadrupole interaction dominates (or $\eta_1\gg 1$ and $\eta_3\gg 1$), both A and C are positive and $\beta_1=\beta_3=0$ is the absolute minimum of the energy. So this region of the parameter space corresponds to the octupole/dipole vibrational phase.

(ii) $B^2-AC>0$: Increasing the octupole and dipole strengths while reducing the one-body energies will eventually change the sign of the discriminant. The energy surface then has a saddle shape and unstable against deformation in the β_1-β_3 plane. The absolute minimum of the energy occurs at a point with $\beta_1>0$ and/or $\beta_3>0$. This region of the parameter space complements the case (i) and corresponds to the octupole/dipole deformed phase.

(iii) $B^2-AC=0$: The surface defined by this condition in the parameter space clearly defines the critical region between the vibrational and deformed phases. We will not discuss further the implications of the critical condition on the model parameters and derive relations among them for the onset of octupole/dipole deformation because, as is shown below, this is a chimerical phase transition that disappears after PP.

To see the effect of PP on the shape-phase transition, we expand the $spdf$-IBM energy surface (35) with $\pi=+1$ for small β_1 and β_3

$$\begin{aligned}
&E_{+spdf}(\beta_1,\beta_2,\beta_3)\\
&\quad=E_{sd}(\beta_2)-2N^2\kappa_2(1+\beta_2^2)^{-2}\{\zeta_1[(1+\overline{\chi}_1\beta_2)\beta_1\\
&\qquad+\overline{\chi}_1'\beta_2\beta_3]^2+\zeta_3[\overline{\chi}_3'\beta_2\beta_1+(1+\overline{\chi}_3\beta_2)\beta_3]^2+\cdots\}.
\end{aligned}\tag{48}$$

Comparing Eq. (48) with Eq. (46), it is seen that contributions from all the positive parity operators have vanished after PP, and only the dipole and octupole interaction terms are left behind at the quadratic level. It is clear from Eq. (48) that the presence of any nonzero strength of the dipole or octupole interactions will cause an instability in the energy surface at $\beta_1=\beta_3=0$, leading to a dipole/octupole deformed system. The direction of deformation in the β_1-β_3 plane depends on the relative strengths of the dipole and octupole interactions. In realistic cases, the octupole interaction is much stronger and, therefore, the system will mainly deform along the β_3 axis. Thus the results presented for the sdf-IBM in Fig. 2 provide an approximate picture for the phase transition in the $spdf$-IBM as well.

IV. ONE-PHONON BANDS

So far we have discussed the ground state properties of mixed parity systems with and without PP. However, most of the data on octupole deformation are obtained from the excitation of collective negative parity bands. Here we derive expressions for the excitation energies and transition strengths for the negative-parity bands. Assuming axial symmetry, the one-phonon bands can be written as

$$|\phi_K\rangle=[(N-1)!]^{-1/2}(b^\dagger)^{N-1}b_K^\dagger|0\rangle,\quad b_K^\dagger=\sum_l y_{lK}b_{lK}^\dagger,\tag{49}$$

where $K=0$, 1, 2, 3 for the $spdf$-IBM, and y_{lK} are the mean fields to be determined from the variation of the respective band energies. The normalization of the parity-projected one-phonon bands is given by

$$\mathcal{N}_{\pi K}=\langle\phi_K|P_\pi|\phi_K\rangle=\frac{1}{2}(\mathbf{x}\cdot\mathbf{x})^{N-1}[\mathbf{y}_K\cdot\mathbf{y}_K+\pi r^{N-1}\mathbf{y}_K\cdot\mathbf{y}'_K]. \tag{50}$$

Here the prime on mean fields denotes parity transformation as in Eq. (11). For $K\neq 0$, orthogonality of the one-phonon bands with the ground band is implicit but this is not so for $K=0$, and needs to be enforced by the condition

$$\langle\phi_g|P_\pi|\phi_0\rangle=0, \tag{51}$$

which leads to the following relationship among the mean fields:

$$\mathbf{x}\cdot(\mathbf{y}_0+\pi r^{N-1}\mathbf{y}'_0)=0. \tag{52}$$

For strong coupling, $r\ll 1$, and the orthogonality condition reduces to the familiar $\mathbf{x}\cdot\mathbf{y}_0=0$ between the ground and $K=0$ bands. Then the expression (50) also holds for the normalization of the $K=0$ bands. But in general, it is modified by an additional term

$$\mathcal{N}_{\pi 0}=\frac{1}{2}(\mathbf{x}\cdot\mathbf{x})^{N-1}\left\{\mathbf{y}_0\cdot\mathbf{y}_0+\pi r^{N-1}\mathbf{y}_0\cdot\mathbf{y}'_0 + \frac{N-1}{\mathbf{x}\cdot\mathbf{x}}[(\mathbf{x}\cdot\mathbf{y}_0)^2+\pi r^{N-2}(\mathbf{x}\cdot\mathbf{y}'_0)^2]\right\}. \tag{53}$$

A. One-phonon band energies

The expectation value of the Hamiltonian (5) in the one-phonon bands (49) can be evaluated in a straightforward manner. For the $K\neq 0$ bands, the energy expressions are relatively simple, given by

$$\begin{aligned}E_{\pi K}&=\frac{1}{\mathcal{N}_{\pi K}}\langle\phi_K|HP_\pi|\phi_K\rangle,\\ &=\frac{(\mathbf{x}\cdot\mathbf{x})^{N-1}}{2\mathcal{N}_{\pi K}}\Bigg(\sum_l\ \varepsilon_l\Bigg\{[1+\pi(-1)^l r^{N-1}]y_{lK}^2 + \frac{N-1}{\mathbf{x}\cdot\mathbf{x}}[\mathbf{y}_K\cdot\mathbf{y}_K+\pi(-1)^l r^{N-2}\mathbf{y}_K\cdot\mathbf{y}'_K]x_l^2\Bigg\}\\ &\quad-\sum_k\ \kappa_k\frac{N-1}{\mathbf{x}\cdot\mathbf{x}}\Bigg[2(A_kA_{kK}+B_{kK}^2) +2\pi r^{N-2}(A'_kA'_{kK}+B'_{kK}B''_{kK})\\ &\quad+\frac{N-2}{\mathbf{x}\cdot\mathbf{x}}(\mathbf{y}_K\cdot\mathbf{y}_KA_k^2+\pi r^{N-3}\mathbf{y}_K\cdot\mathbf{y}'_KA'^2_k)\Bigg]\Bigg).\end{aligned} \tag{54}$$

Here the various quadratic forms are defined similar to Eq. (16), for example,

$$A_{kK}=\sum_{jl}\ \langle jKl-K|k0\rangle t_{kjl}y_{jK}y_{lK},$$

$$B_{kK}=\sum_{jl}\ \langle jKl0|kK\rangle t_{kjl}y_{jK}x_l, \tag{55}$$

with the prime denoting a parity transformed mean field in the above forms $x'_l=(-1)^l x_l$

$$A'_k=\sum_{jl}\ \langle j0l0|k0\rangle t_{kjl}x_jx'_l,$$

$$A'_{kK}=\sum_{jl}\ \langle jKl-K|k0\rangle t_{kjl}y_{jK}y'_{lK},$$

$$B'_{kK}=\sum_{jl}\ \langle jKl0|kK\rangle t_{kjl}y_{jK}x'_l,$$

$$B''_{kK}=\sum_{jl}\ \langle jKl0|kK\rangle t_{kjl}y'_{jK}x_l. \tag{56}$$

Subtracting the ground state energy from Eq. (54), one obtains the band-excitation energies. For the $K=0$ bands, there are additional terms arising from the nonorthogonality of boson operators as in the case of the normalization (53). These terms typically introduce small corrections to the band energies but because they are lengthy and are not of much interest, they are not given here. (The energies of the $K=0$ bands in the next section are, of course, calculated using the full expressions.)

B. Electric moments and transitions

For even-multipole operators, the static moment of a one-phonon band is given by

$$\begin{aligned}T^\pi_{k0}&=\frac{1}{\mathcal{N}_{\pi K}}\langle\phi_K|T^{(k)}_0P_\pi|\phi_K\rangle\\ &=\frac{(\mathbf{x}\cdot\mathbf{x})^{N-1}}{2\mathcal{N}_{\pi K}}\Bigg[A_{kK}+\frac{N-1}{\mathbf{x}\cdot\mathbf{x}}\mathbf{y}_K\cdot\mathbf{y}_KA_k +\pi r^{N-1}\left(A'_{kK}+\frac{N-1}{\mathbf{x}\cdot\mathbf{x}}\mathbf{y}_K\cdot\mathbf{y}'_KA'_k\right)\Bigg].\end{aligned} \tag{57}$$

The quadratic forms here and in the expressions below are given in Eqs. (55) and (56). For odd-multipole operators, we calculate the transition moment between the positive and negative parity K bands

$$\begin{aligned}T^{+-}_{k0}&=[\mathcal{N}_{+K}\mathcal{N}_{-K}]^{-1/2}\langle\phi_K|P_+T^{(k)}_0P_-|\phi_K\rangle,\\ &=\frac{1}{2}[\mathcal{N}_{+K}\mathcal{N}_{-K}]^{-1/2}(\mathbf{x}\cdot\mathbf{x})^{N-1}\left[A_{kK}+\frac{N-1}{\mathbf{x}\cdot\mathbf{x}}\mathbf{y}_K\cdot\mathbf{y}_KA_k\right].\end{aligned} \tag{58}$$

Finally we calculate the intrinsic matrix elements for the excitation of the K bands assuming the same multipole operators for electric transitions as those employed in the Hamiltonian

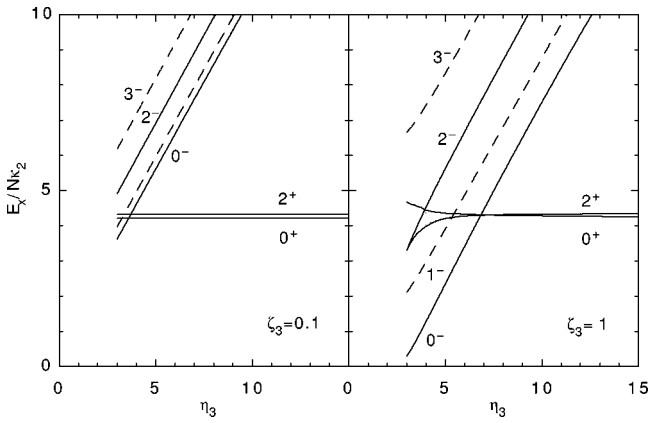

FIG. 3. Dependence of the excitation energies of single-phonon bands (in units of $N\kappa_2$) on the octupole boson energy $\eta_3 = \varepsilon_3/N\kappa_2$. On the left panel, $\zeta_3 = 0.1$ and on the right, $\zeta_3 = 1$. The other parameters are $\chi_- = 0.5$, $\eta_1 = 15$, and $\zeta_1 = 0.1$.

$$\langle \pi K | T^{(k)}_K | \text{g.s.} \rangle = [\mathcal{N}_{\pi K}\mathcal{N}_{\text{g.s.}}]^{-1/2} \langle \phi_K | P_\pi T^{(k)}_K P_+ | \phi_{\text{g.s.}} \rangle,$$
$$= \frac{\sqrt{N}}{4}[1+(-1)^k\pi][\mathcal{N}_{\pi K}\mathcal{N}_{\text{g.s.}}]^{-1/2} \times (\mathbf{x}\cdot\mathbf{x})^{N-1}(B_{kK} + r^{N-1}B'_{kK}). \quad (59)$$

Clearly only the bands with $\pi = (-1)^k$ have non-zero transitions to the ground state. The result in Eq. (59) does not incorporate the time reversal invariance, which is important in comparison with experimental results in the lab frame. This is achieved simply by multiplying the matrix elements for $K \neq 0$ states by a factor of $\sqrt{2}$ in Eq. (59) [32].

As in the case of the band-energies, there are extra terms for the $K=0$ bands that have not been included in the above matrix elements. Nevertheless the systematic studies in the next section are carried out using the full expressions.

V. SYSTEMATIC STUDIES

In this section, we present systematic studies of the parameter dependence of band-excitation energies and transition matrix elements. The results are contrasted with the experimental data in the rare-earth and actinide nuclei with a view of determining the appropriate ranges of model parameters that can be employed in detailed studies of negative-parity bands in specific nuclei. The key parameters are the single boson energies (η_1, η_3) for the p and f bosons and their coupling strengths (ζ_1, ζ_3). We also consider the effect of χ_- as it can expedite mixing of the negative parity bosons in the ground state band. Unless otherwise stated, the $\overline{\chi}$ parameters are taken from the adapted values in Table I. The d-boson energy is fixed as $\eta_2 = 1.5$ throughout as found from the fits to the β and γ bands [24]. The results are presented such that they are independent of the number of bosons N and the quadrupole coupling strength κ_2.

A. Band excitation energies

In Fig. 3, we plot the excitation energies for the single-phonon bands as a function of the f boson energy. On the left panel, $\zeta_3 = 0.1$, which represents the weak coupling of octupole bosons appropriate to the rare-earth region. On the right, $\zeta_3 = 1$, representing the strong coupling observed in the actinide nuclei. The p bosons are assumed to be weakly coupled in these figures ($\eta_1 = 15$ and $\zeta_1 = 0.1$). Except in the case of extreme mixing, η_3 is seen to have no influence on the β and γ-band energies. The negative-parity bands exhibit a linear dependence in both cases, suggesting that the f boson energy would be best determined from their center of energy. A linear correlation between the octupole centroids and neutron number has been observed in rare earths and actinides [7]. Thus the f boson energies can be determined in a rather unique way for all nuclei with octupole excitations. Comparison of the two panels indicates that increasing the octupole coupling strength leads to a larger splitting among the octupole bands. On the right panel, $K = 0^-$ band is seen to merge with the ground state, signalling the onset of rigid octupole deformation. This behavior is more likely to be induced by an increase in octupole coupling rather than a reduction in the f-boson energy. This is shown in Fig. 4, where the band-excitation energies are plotted as a function of ζ_3 for a fixed $\eta_3 = 3$. With increasing ζ_3, the octupole bosons steadily mix in the ground state and the $K = 0^-$ band comes down. For $\zeta_3 > 1$, the two bands merge and the condensate becomes a mixture of positive and negative-parity bosons. In the Ra and Th nuclei, the $K = 0^-$ bands do not quite merge with the ground state band [21], indicating that $\zeta_3 < 1$ in these nuclei.

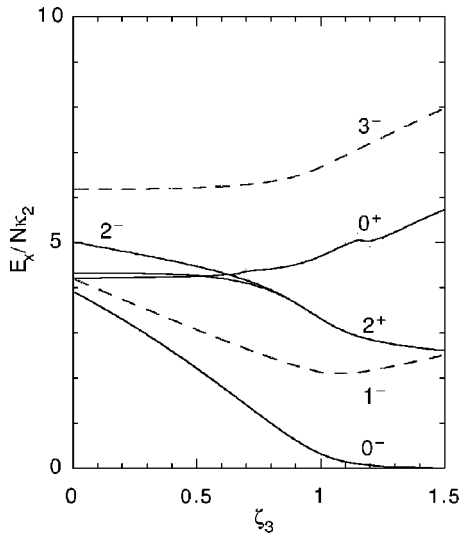

FIG. 4. Dependence of the excitation energies of single-phonon bands on the octupole coupling strength $\zeta_3 = \kappa_3/\kappa_2$ for a fixed $\eta_3 = 3$. The other parameters are the same as in Fig. 3.

A question of considerable interest for applications of the sdf-IBM with one f boson is the number of f bosons in the ground and $K = 0^-$ bands. For $\zeta_3 < 0.5$, these numbers are as expected from the octupole vibrations, that is, $\langle \hat{n}_f \rangle \approx 0$ for the ground band and 1 for the $K = 0^-$ band. However, with further increase in ζ_3 the number of f-bosons rapidly increase becoming $\langle \hat{n}_f \rangle \approx 2$ for both bands around $\zeta_3 \approx 1$. Thus the restriction of the negative-parity bosons to 1 is not a good approximation in regions of stable octupole deformation.

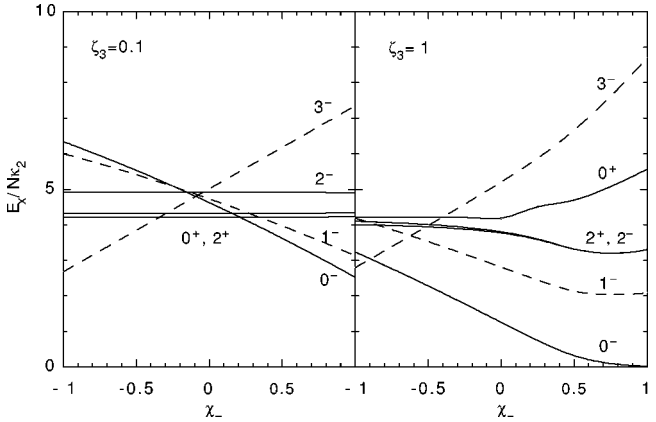

FIG. 5. Dependence of the excitation energies of single-phonon bands on the parameter χ_- in the quadrupole operator. $\eta_3=3$, $\zeta_3=0.1$ on the left and 1 on the right. The other parameters are the same as in Fig. 3.

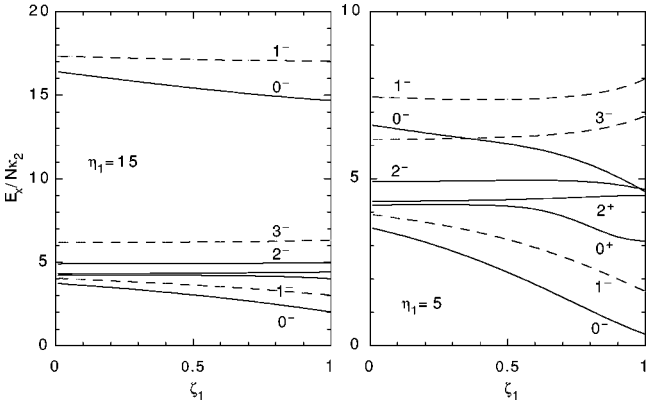

FIG. 6. Similar to Fig. 4 but for $\zeta_1=\kappa_1/\kappa_2$ when $\eta_3=15$ (left) and $\eta_3=5$ (right). The other parameters are $\chi_-=0.5$, $\eta_3=3$, and $\zeta_3=0.1$.

The ordering of the negative parity bands changes with increasing neutron number in both rare earth and actinide nuclei. In sdf-IBM with one f boson, this behavior is described by including an exchange interaction between the d and f bosons [6,7]. As shown in Fig. 5, the ordering of the bands from $K=0^-$ to 3^- can be reversed by changing the sign of the χ_- parameter in the case of the weak octupole coupling ($\zeta_3=0.1$). However, other orderings such as 1^-, 0^-, 2^- observed in ^{172}Yb, cannot be obtained within the restricted parameter set employed in this work. Thus, in studies of specific nuclei, one needs to consider variations in the χ parameters from the SU(3) values in order to reproduce such details as ordering of the band heads.

We next consider the effect of the p-boson parameters. In the previous figures, p bosons were weakly coupled, and the corresponding $K=0^-$, 1^- bands were outside the figures. The p-boson energy has a similar effect on the band energies as the f-boson energy shown in Fig. 3, namely, the energies of the $K=0^-$, 1^- bands associated with the p bosons linearly increase with η_1 while the others remain nearly flat (not shown). Of more interest is the effect of the dipole coupling strength in the case of high ($\eta_1=15$) and low-lying ($\eta_1=5$) p-boson energies. As shown in Fig. 6, in the former case, the f and p boson bands remain well separated and remain rather pure even at the strong coupling limit. In the latter situation, the bands start mixing with increasing ζ_1 and cannot be identified as being p or f-boson band for $\zeta_1>0.5$. For example, the second $K=0^-$ band has more f bosons than p bosons in the condensate near $\zeta_1=1$.

B. $E1$ and $E3$ transitions

When the p bosons are weakly coupled (i.e., $\eta_1\approx 15$), the octupole-boson bands remain rather pure, and the f-boson energy has almost no effect on the $E3$ transition strengths to the ground state as long as they are not very strongly coupled. In the strong coupling limit ($\zeta_3\approx 1$), the $E3$ $K=0^-\rightarrow 0_{\text{g.s.}}$ transition strength rapidly increases as the $K=0^-$ band comes down with decreasing η_3. But the other $E3$ transitions show little dependence on η_3 even in the strong coupling limit. Thus a more relevant parameter for studying the $E3$ systematics is ζ_3, which is shown in Fig. 7 (left panel). In the weak coupling limit, the $E3$ transition strengths from the $K=0^-$, 1^-, 2^- bands are all similar but that from the 3^- band is much smaller (mostly unobserved). With increasing octupole coupling, the strength of the $E3$ transition from the $K=0^-$ band increases relative to the others. These features are in broad agreement with the observed $B(E3)$ systematics in the rare-earth and actinide nuclei, and gives support to the values of the χ parameters chosen in this work. Obviously, one has to fine tune the value of χ_3 parameter in the $E3$ operator in order to reproduce the variation in the observed distribution of strengths among the octupole bands. The dependence of the $E3$ matrix elements on χ_3 are shown on the right panel of Fig. 7. Here the transition from $K=2^-$ band remains independent of χ_3 because the corresponding Clebsch-Gordon coefficient in Eq. (59) vanishes.

The results in Fig. 7 suggests an alternative explanation for the nonobservation of the $K=3^-$ bands in experiments: rather than being much higher in excitation energy, they may

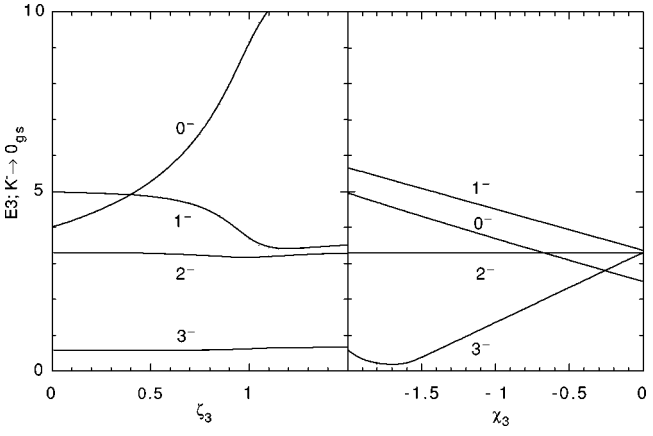

FIG. 7. Intrinsic matrix elements for $E3$ transitions from the negative-parity bands to the ground state. Absolute values of the matrix elements are plotted as a function of the octupole coupling strength ζ_3 (left) and χ_3 for $\zeta_3=0.1$ (right). The other parameters are the same as in Fig. 4.

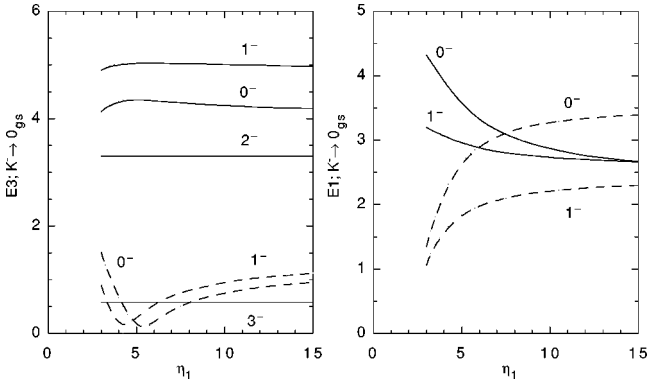

FIG. 8. Dependence of the $E3$ (left) and $E1$ (right) transitions on the p-boson energy. The p-boson bands are indicated by the dashed lines. Here $\eta_3=3$, $\zeta_3=0.1$, $\zeta_1=0.1$, and the other parameters are the same as in Fig. 7.

have much smaller $E3$ transition strengths to the ground state and thus not seen in Coulomb excitation experiments. This also provides another incentive for avoiding the positive range of the χ_3 parameter because they would lead to large $B(E3)$ values for the excitation of the $K=3^-$ bands (besides leading to nonaxial shapes).

We next discuss the influence of the p bosons on the $E1$ and $E3$ systematics. Variations in the p-boson coupling strength have little effect on the $E1$ and $E3$ transitions from the negative-parity bands, and therefore we will not consider them further here. The p-boson energy, on the other hand, has some influence on the $E1$ and $E3$ transitions as shown in Fig. 8. The $E3$ transitions from the $K=0^-$, 1^- bands associated with the p bosons are seen to be much weaker, and similar in strength to that from the unobserved $K=3^-$ band. This suggests a fundamental difficulty in identification of collective dipole bands from Coulomb excitation experiments regardless of whether such bands are low lying (in the region of octupole excitations) or high lying. Curiously, the $E3$ matrix elements vanish for $\eta_1\approx 5$, so the dipole bands would be even more elusive were they to lie just above the octupole bands. The situation with respect to the strengths of transitions from the p boson $K=0^-$, 1^- bands is more promising in the case of $E1$ transitions (Fig. 8, right panel). As long as the p- and f-boson energies are not degenerate, the matrix elements for all the $E1$ transitions have similar magnitude. This suggests that measurement of $E1$ transitions from the $K=0^-$, 1^- bands are likely to be more helpful in identification of the collective dipole excitations. Data on absolute $B(E1)$ values are meager and it is not easy to confirm the appropriateness of the chosen $E1$ operator from the experimental systematics. Nevertheless, the measured $B(E1)$ values in ^{156}Gd from the $K=0^-$, 1^- octupole bands are consistent with the results shown in Fig. 8 [33].

VI. CONCLUSIONS

We have developed a mean field formalism for the study of negative-parity states within the $spdf$-IBM. The results are employed in studying the octupole shape-phase transitions in quadrupole deformed nuclei. An interesting result is the important role parity projection plays on the octupole shape transitions, completely changing the shape-phase diagram compared to the unprojected case. This is to be contrasted with the onset of quadrupole deformation, where the mean field results change little (of order $1/N$) after angular momentum projection. The mean field results allow a systematic study of excitation energies of negative-parity bands, and $E1$ and $E3$ transitions from them. The results are in broad agreement with the experiments, indicating that the simplified parametrization suggested in this work may provide a good starting point for detailed studies of negative-parity states in individual nuclei. Regarding the dipole collective bands, we have found that the observables exhibit a general insensitivity towards the p boson parameters. Thus it would be difficult to make any suggestions about the possible location of the dipole bands from the systematics alone. According to our results, the best signature for the dipole excitations would be the observation of $E1$ transitions from a second set of $K=0^-$, 1^- bands that have similar strengths to those from the first set that have octupole nature.

ACKNOWLEDGMENTS

The authors thank the Australian Academy of Science and Japan Society for Promotion of Science for supporting this work through the Bilateral Exchange Program.

[1] S. G. Rohozinski, Rep. Prog. Phys. **51**, 541 (1988).
[2] I. Ahmad and P. A. Butler, Annu. Rev. Nucl. Part. Sci. **43**, 71 (1993).
[3] P. A. Butler and W. Nazarewicz, Rev. Mod. Phys. **68**, 349 (1996).
[4] F. Iachello and A. Arima, *The Interacting Boson Model* (Cambridge University Press, Cambridge, 1987).
[5] F. Iachello and A. Arima, Ann. Phys. (N.Y.) **111**, 201 (1978).
[6] A. F. Barfield, B. R. Barrett, J. L. Wood, and O. Scholten, Ann. Phys. (N.Y.) **182**, 344 (1988).
[7] P. D. Cottle and N. V. Zamfir, Phys. Rev. C **54**, 176 (1996); **58**, 1500 (1998).
[8] N. V. Zamfir and D. Kusnezov, Phys. Rev. C **63**, 054306 (2001).
[9] J. Engel and F. Iachello, Phys. Rev. Lett. **54**, 1126 (1985); Nucl. Phys. **A472**, 61 (1987).
[10] F. Catara, M. Sambataro, A. Insolia, and A. Vitturi, Phys. Lett. B **180**, 1 (1986).
[11] T. Otsuka, Phys. Lett. B **182**, 256 (1986).
[12] C. S. Han, D. S. Chun, S. T. Hsieh, and H. C. Chiang, Phys. Lett. **163B**, 295 (1985).
[13] T. Otsuka and M. Sugita, Phys. Lett. B **209**, 140 (1988).
[14] D. Kusnezov and F. Iachello, Phys. Lett. B **209**, 420 (1988).
[15] H. Y. Ji, G. L. Long, E. G. Zhao, and S. W. Xu, Nucl. Phys. **A658**, 197 (1999).
[16] C. E. Alonso *et al.*, Nucl. Phys. **A586**, 100 (1995).

[17] V. S. Lac and I. Morrison, Nucl. Phys. **A581**, 73 (1995).
[18] A. F. Diallo, B. R. Barrett, P. Navratil, and C. Gorrichategui, Ann. Phys. (N.Y.) **279**, 81 (2000).
[19] J. F. Smith *et al.*, Phys. Rev. Lett. **75**, 1050 (1995).
[20] J. F. C. Cocks *et al.*, Phys. Rev. Lett. **78**, 2920 (1997).
[21] J. F. C. Cocks *et al.*, Nucl. Phys. **A645**, 61 (1999).
[22] I. Wiedenhöver *et al.*, Phys. Rev. Lett. **83**, 2143 (1999).
[23] A. Aprahamian (private communication).
[24] S. C. Li and S. Kuyucak, Nucl. Phys. **A604**, 305 (1996).
[25] F. Iachello and A. Zilges (private communication).
[26] M. Sugita, T. Otsuka, and P. von Brentano, Phys. Lett. B **389**, 642 (1996).
[27] J. N. Ginocchio and M. W. Kirson, Nucl. Phys. **A350**, 31 (1980).
[28] S. Levit and U. Smilansky, Nucl. Phys. **A389**, 56 (1982).
[29] A. E. L. Dieperink and O. Scholten, Nucl. Phys. **A346**, 125 (1980).
[30] S. Kuyucak and I. Morrison, Appl. Phys. (N.Y.) **181**, 79 (1988).
[31] S. Kuyucak, Phys. Lett. B **466**, 79 (1999).
[32] A. Bohr and B. R. Mottelson, *Nuclear Structure* (Benjamin, Reading, MA, 1975), Vol. 2.
[33] H. H. Pitz, U. E. P. Berg, R. D. Heil, U. Kneissl, R. Stock, C. Wesselborg, and P. von Brentano, Nucl. Phys. **A492**, 411 (1989).